EDU Journal of International Affairs and Research (EJIAR), ISSN: 2583-9993
Volume 3, Issue 3, July-September, 2024, Available at: https://edupublications.com/index.php/ejiar

Effect of Iron Doping of Structural and Magnetic Activity on Iron Aluminate Nano-Materials by Microwave Irradiated Chemical Co-Precipitation Protocol

Seema[1], Sunita Dahiya[2], Rajesh Sharma[3*]

[1]Research Scholar, Baba Mastnath University, Rohtak-124001, India
[2]Faculty in Physics, Baba Mastnath University, Rohtak-124001, India
[3]Faculty in Physics, MNS Govt. College, Bhiwani - 127021, India

[#]**Corresponding Author-** rkkaushik06@gmail.com

ABSTRACT

In present work designates the preparation of nanocrystalline Iron dopped Alumina nanoparticles with general formula $Al_2Fe_2O_6$-μ prepared by microwave irradiated chemical co-precipitation protocol. The structural (XRD and FTIR), morphological (FESEM, HRTEM) and magnetic properties of the products were characterized. The XRD results explores that the prepared nano-particles lies in nano-region and obey hexagonal crystalline nature. The FTIR spectrum of 10% Iron Oxide incorporated Aluminium Oxide, calcined at various temperatures 200°C, 400°C and 600°C for 2hrs.The IR results reveals that broad band spanning 3500 cm- to 3330 cm-1 and another wide band between 1700 cm-1 and 1500 cm-1 were corresponds to hydroxyl ion vibration of water present in atmosphere moisture. The peaks at 827 cm-1 and 504 cm-1 are associated with metal oxide (MOs) vibrations, such as Al-O-Al in the Al_2O_3 and O-Fe-O of Fe_2O_3 nanostructures. The FESEM images of Fe_2O_3 dopedAl_2O_3 nano-structured substances calcined at 600°C/2hrs that substance are homogenous in size, cluttered in macrocosm and truncated spherical in contour. Observation of the HRTEM images explores that the dimensions of the nano-structured substances lies in confine of 30 nm to 35 nm and aggregate grain size determined out 32 nm. There upon the HRTEM summary are in accordance with those of XRD outcomes.

Keywords: Iron aluminate, Debye-Schererr, VSM, FTIR, FESEM and HRTEM.

INTRODUCTION

The science and technology of nanosized particles are extensive and interdisciplinary area that comprehended various branch of science i.e. physics, bio-chemistry, materials science, electronics, engineering and medical science etc with aspects of mutually dependent together. The applicability of such materials are highly sensitive with size of material and also different chemical and physical property such as oxidation state, chemical state, type of bonding between particles, color, binding energy, melting and boiling point etc. the reason ascribed for such enhancement are transformation of classical to quantum (at nanoscale) state of particulates. Among all the reassuring nano-dimensioned materials/substances, Iron (Fe)-based ones, despite being relatively underutilized, are rich in implied promise. Iron Oxide has already been used in a variety of fields since the 19th century for the treatment /cure of bacterial illnesses, but its use has declined since the mid-twentieth century due to the occurrence of flexible Iron encephalitis (viral infection) in France and Australia.

Nevertheless, Iron-based medicinal products such as Iron subsalicylate, bio-active conjugates, colloidal Iron sub-citrate, and others are still used for gastrointestinal issues treatment/cure. Researchers are now very interested in nanotechnology due to its attractive features in a variety of domains, including huge surface to volume ratio, electrical and optical properties, etc. The primary causes of the significant changes in particle characteristics at the nanoscale are its large surface to volume ratio (S/V), the consequence of quantum confinement, and the modular photonic band gap. Nano-Crystallites are nanoparticles with a finely organized atom/ion configuration.

Experimental Details

In the procedure of synthesis of Iron Oxide doped Aluminium Oxide nanocomposites were prepared by utilizing microwave-modified chemical co-precipitation modus. The main content for preparing NPs are ($Al(NO_3)3.9H_2O$) of (THOMAS BAKER) having molecular weight 213 and Iron Nitrate ($Fe(NO_3)_3.9H_2O$) of Himedia Chemicals limited having molecular weight 403.99 was utilized [191].The above-said constituents with suitable concentration were dissolved in 200ml doubly distilled water.The prepared solution was kept on a magnetic stirrer for half an hour to prepare a transparent homogenous solution, and the pH value was measured using a pH meter, which was 2.6, after which the solution of ammonia was added drop-by-drop to keep the pH of the resulting solution around 9 and the bluish colour of the solution was observed. Some amount of heat was released during the solution preparation which explores that the solution possesses exothermic reaction. After addition of ammonia solution was again kept on magnetic stirrer and stirred for duration of one hour and after it the precipitated solution was kept for aging process for 24 hours so that the particulates will settle down [192]. Now water above from the precipitates was drained out using pipette and the collected precipitates were filtered using very small pore size Whatman filter papers and washed with de-ionized water and ethanol of MERCK a number of times. After washing and filtration process obtained specimens were kept in microwave oven for extracting out water content present within the precipitates. Now these specimens were put up in china disc and kept in muffle furnace at different – different ignition temperatures (200^oC, 400^oC &600^oC) for two hours and after it the ignited samples were grinded in form of fine powder using agate mortar and powdered form of these nano-stuffs filled in air tight containers so that these can be utilized for further characterization.

The prepared specimens' structural, morphological, optical, magnrtic and electronic properties were investigated using the XRD, IR, VSM spectroscope, FESEM, and **Results and Discussion**

Structural Characterization:
To allocate the framework of ignited specimen by using X-ray diffractometer with copper (CuK_α)radiation (λ = 1.5408 Å) in the confine of 10^0–80^0 the powder sample studies using X-rays have been accomplished. The XRD designs of various iron oxide doped Aluminium Oxide nano-sized stuff ignited at 600^oC temperature for 2 hours are exhibited in **Figure-1**

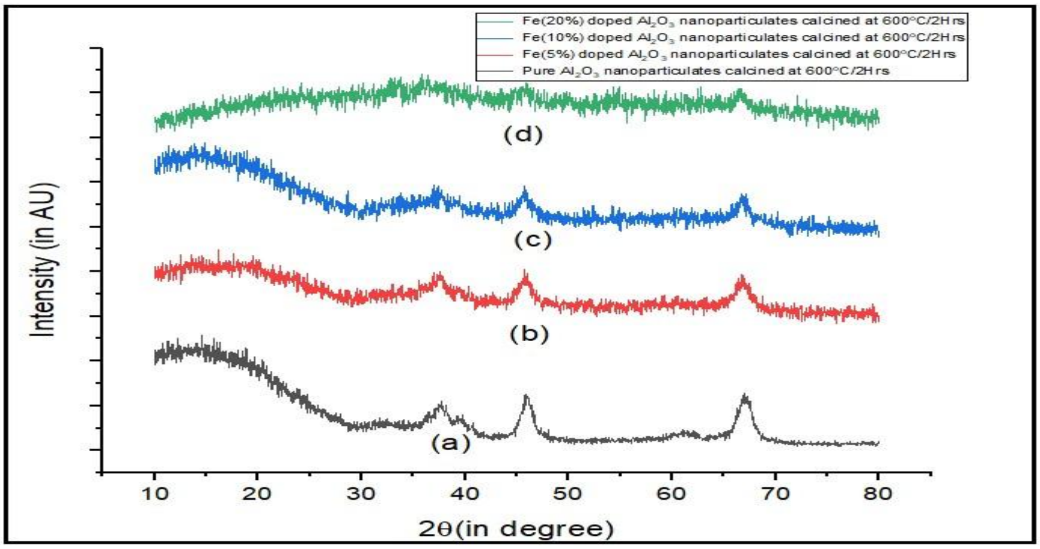

Figure-1: XRD plot of Fe doped Al_2O_3 nano stuffs calcination at temperature 600^oC for 2 hrs (a) Pure Al_2O_3 (b) Al_2O_3 – Fe_2O_3(5%) (c) Al_2O_3 – Fe_2O_3(10%) (d) Al_2O_3 – Fe_2O_3(20%).

The X –Ray diffraction spectrum of various calcined samples of Fe doped Alumina were examined through graph and the result shows that the most intense alps of various dopant concentration samples were occurred at position of 2Θ ≈ 45.15$^{\mathbf{o}}$ and other significant peaks at position 2Θ ≈ 41.23$^{\mathbf{o}}$. The above said peaks match with JCPDs card no, 71-1123 XRD results confirmed the complete formation of α-Al_2O_3. The study reflect that the position of most intense alps were more or less same. However, the FWHM value and intensity of peaks observed with changes with dopant concentration. Moreover, the 36.651°, 46.88°, 65.516°,66.16° additional peaks were found and analogous to JCPDs card no. 65-3107 of Fe_2O_3 . the result of study indicates that Fe^{3+} replace the Al^{3+} and successfully incorporated in Al_2O_3 structure and resulted change with intensity of peaks.

Table-1: Crystallite size of Iron Oxide (5%, 10% and 20%) incorporated Aluminium Oxide nano-stuffs annealed at temperature 600oC for duration of two hours.

Sr. No.	Dopant concentration (%)	2Θ (Degrees)	FWHM (Radians)	Crystallite size (nm)
1	Fe 5% doped Al_2O_3	46.09	0.425	29.35 nm
2	Fe 10% doped Al_2O_3	45.73	0.605	33.17 nm
3	Fe 20% doped Al_2O_3	45.88	0.583	34.38 nm
4	Pure Al_2O_3	45.87	0.525	34.56 nm

The study reflect that the position of most intense alps were more or less same. However, the FWHM value and intensity of peaks observed with changes with dopant concentration. Moreover, the 36.651°, 46.88°, 65.516°,66.16° additional peaks were found and analogous to JCPDs card no. 65-3107 of Fe_2O_3 . the result of study indicates that Fe^{3+} replace the Al^{3+} and successfully incorporated in Al_2O_3 structure and resulted change with intensity of peaks.

FTIR Spectroscopy analysis

The IR spectroscopy were used to identified the group/ contamination particles/ other entities present in the samples. The transmittance rate were noted with wave number of radiation incident on samples ranging from 400-4000 cm^{-}1.The FTIR electromagnetic spectrum of synthesized specimen of Fe_2O_3(5%, 10% and 20%) doped Al_2O_3 nano-sized stuff ignited at 600^0C for 2hrs. The IR data were represented in graphs as shown in Figure-2 and shows various vibration peaks against hydroxyl group and O-M-O vibration.

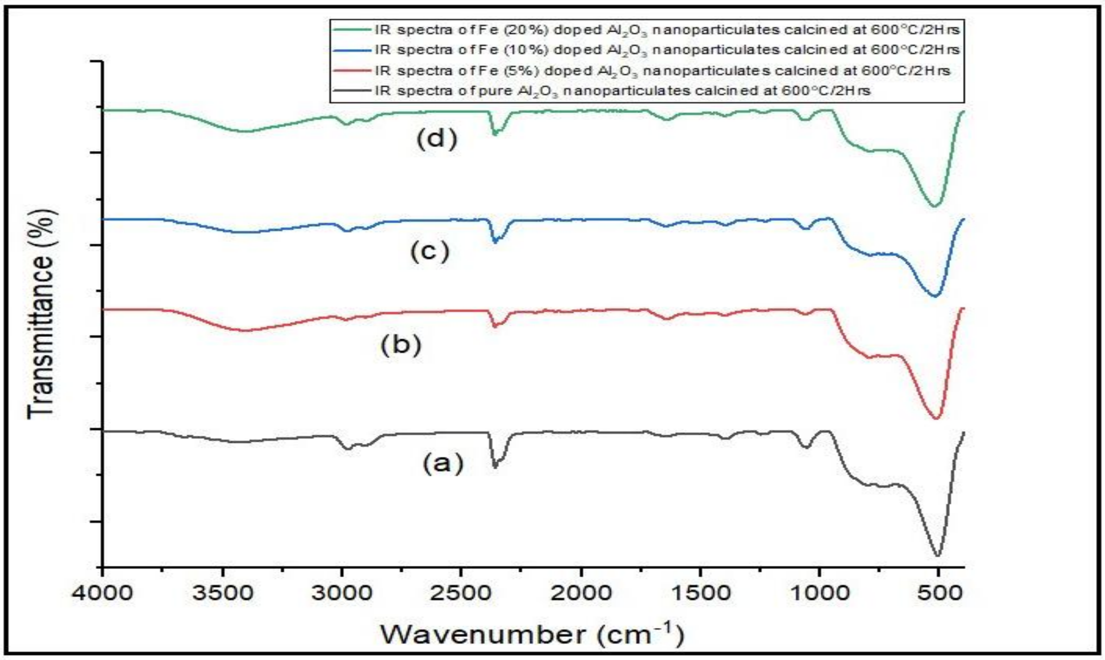

Figure - 2: FTIR Spectra ofZincOxide dopedAl_2O_3 nano-sized stuff with various molar concentrations ignited at 600^0C for 2 hours (a)Al2O3 pure (b)ZnO -Al_2O_3(5%) (c) ZnO -Al_2O_3 (10%) (d) ZnO-Al_2O_3(20%)

For specimens calcined at 600°C for 2 hours with varying Fe_2O_3 dopant concentrations (5%, 10%, and 20%), peak intensities improved and peak positions shifted slightly. The IR peaks observed for each doping concentration were (3402, 1622, 600, and 530)cm^{-1} for 5% doping, (3446, 3341, 1612, 845, 582, and 522)cm^{-1} for 10% doping, and (3419, 1622, 582, and 512)cm^{-1} for 20% doping. Broad bands were observed around 3500-3330 cm-1 and 1700-1400 cm^{-1}, attributed to -OH group vibrations and potentially water content in the surroundings. The peak at 1300 cm^{-1} is likely due to CO_2 and NO_2 adsorption from the surroundings and nitrate salt used in sample preparation. Peaks at 582 cm^{-1} and 512 cm^{-1} are associated with Metal Oxide vibrations like Al-O-Al in Al_2O_3 nano-materials. Investigation reveals that transmittance values increase with higher calcination temperatures.

VSM Analysis

The magnetic properties of various samples were explored through deploying vibrating sample magnetometer tools and the applied field ranges were taken from 0-10,000 Os. In present work the various calcined samples of iron (Fe) 5%,10%,20% doped alumina nanocrystalline were studied through vsm tool and result were compare with pure alumina sampled calcined at 600°C for 2 hrs. The data received from lab CEERI Pilani.were represented in various calculations.The preusal of various calculations representation show that the particles are more or less ferromagnetic in nature with small hysteresis loss.

Sr. No.	Sample Name	Saturation Magnetization(10-3	Coercive Field (in Hc Oe)	Maximum Permeability (in 10^{-6}	Max. energy loss(inMGsOe)
1	Al Pure	74.653	105.673	97.703	14.215
2	Fe 5%	73.400	59.483	102.701	8.096
3	Fe10%	93.382	64.799	119.667	8.591
4	Fe20%	66.367	61.833	60.763	7.923

EDU Journal of International Affairs and Research (EJIAR), ISSN: 2583-9993
Volume 3, Issue 3, July-September, 2024, Available at: https://edupublications.com/index.php/ejiar

VSM graph of pure Al_2O_3 nano-particulates calcined at 600°C of doped Fe (5%, 10%, 20%) calcined at 600°C.

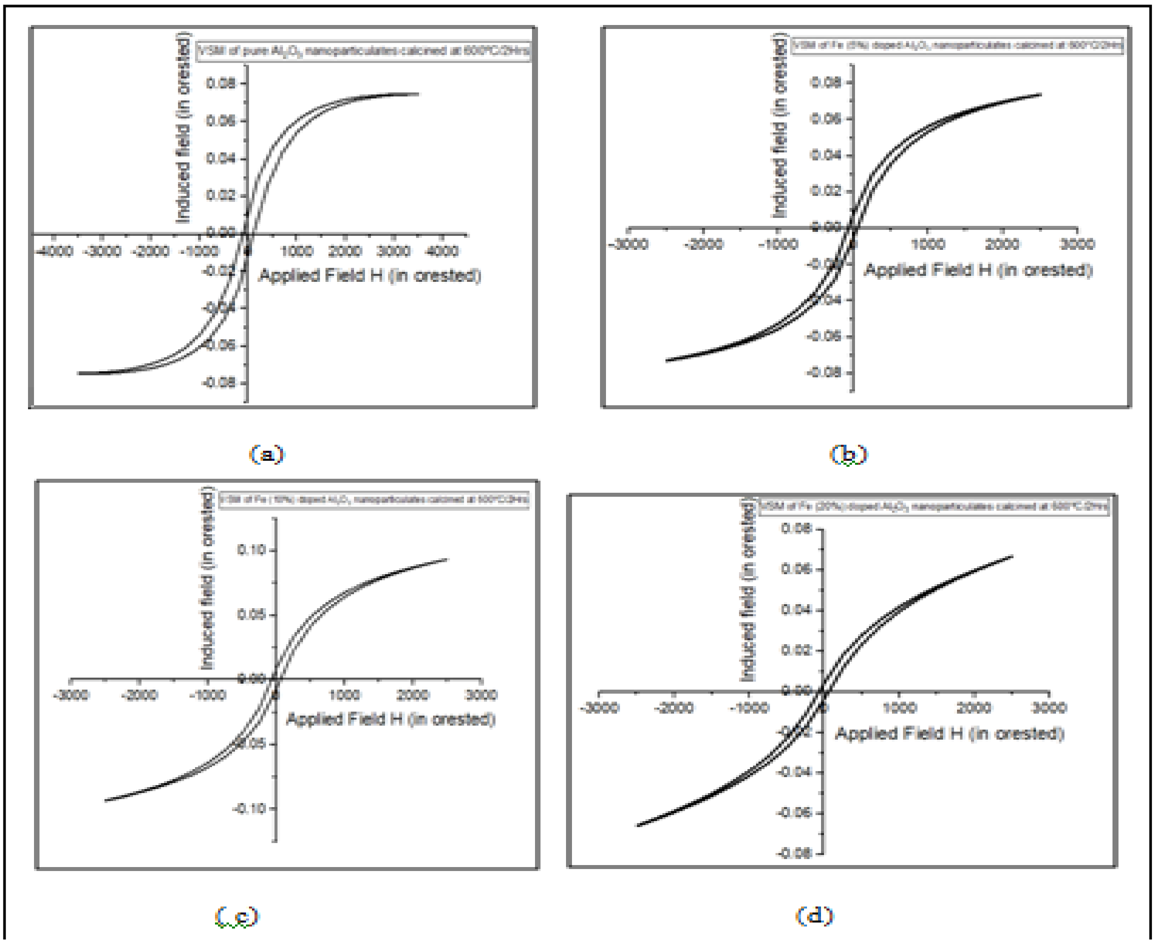

High Resolution Transmission Electron Microscopy (HRTEM) investigation

HRTEM micro-graphs of Iron doped Al_2O_3 nano-composites with concentration 10% ignited at 600 ^{0}C for 2 hours were exhibited in figure-3**.**

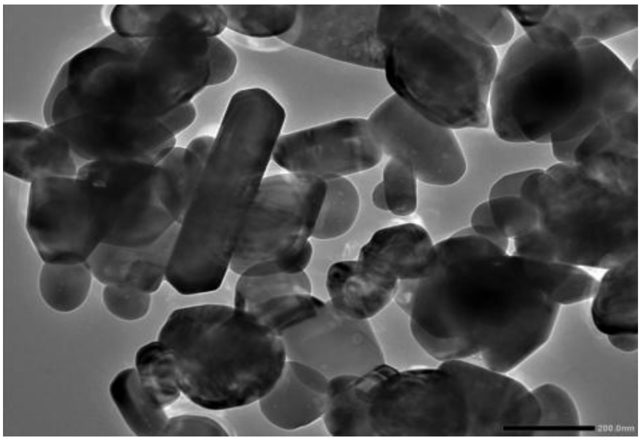

Figure-3: HRTEM image of 10% Fe_2O_3-Al_2O_3 nano-stuffs ignited at temperature 600°C for duration of two hours

Investigation of the images indicates that the nanostructured materials exhibit dimensions confined within 30 nm to 35 nm, with an aggregate grain size determined to be 32 nm.

The summary derived from high-resolution transmission electron microscopy (HRTEM) aligns closely with the results obtained from X-ray diffraction (XRD).

Field Emission Scanning Electron Microscopy (FESEM) study

The scanning of sample through electron microscopy images of ZnO doped Al_2O_3nano-sized stuff ignited at 600 ^{0}C for 2 hours were more or less similar to typical scanning of sample through electron microscopy. Micrograph of ZnO doped Al_2O_3 (10%) nano-composites ignited at 600^{0}C for 2 hours is exhibited in Figure-4**.**

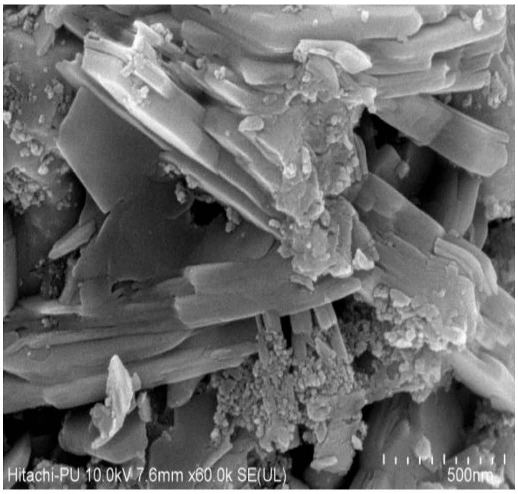

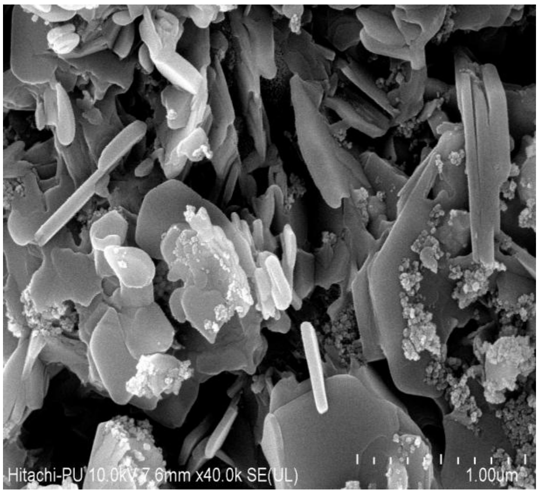

(a) **(b)**

Figure -4: FESEM image of 10% Fe_2O_3 doped Al_2O_3 nano-stuffs ignited at temperature (a) 400^{o}C (b)600^{o}C for 2 hrs

The examination of images revealed that the nanostructured material samples were inherently polycrystalline. Notably, these samples exhibited distinct variations in transmittance and reflectance, likely attributed to the integration of Fe++ ions into the Al_2O_3 lattice. Furthermore, the representative FESEM images depicted the materials as homogeneously sized, macroscopically cluttered, and possessing either truncated spherical contours or crepe-like formations.

CONCLUSIONS

The nano-sized stuff of Fe_2O_3 doped Al_2O_3 having various concentrations of 5%, 10% and 20% of the Fe_2O_3 has been assembled by Micro-wave treated co-precipitation advance synthesis protocols. The conclusions of HRTEM assist the XRD sequels grain size approximate to 30 to 35 nm. The Perusal of HRTEM images exhibit that the size of all ignited Fe_2O_3 dopped Al_2O_3 nano-networked specimen lies in a confine of 30 nm to 35 nm and 2-D nanosheets were in formation. The FTIR Spectra of the ignited nano networked stuff of Fe_2O_3 doped Al_2O_3 containing concentration of 5%, 10% and 20% is exhibiting the Alps(peaks) at 3446, 3341, 1612, 864cm^{-1}, 673cm^{-1}, which are similar to the alps(peaks) as appeared in Fe_2O_3 nano-flecks. Peaks at 582 cm^{-1} and 512 cm^{-1} are associated with Metal Oxide vibrations like Al-O-Al in Al_2O_3 nano-materials.

REFERENCES

[1]. Dwivedi, S. and Biswas, S. (2018a) ‘Enhanced magnetoresistance in pulsed laser deposited stable chromium oxide thin films’, Thin Solid Films, 655, pp. 13–21. doi:10.1016/j.tsf.2018.03.093.

[2]. Chahar, R. and Das Mukherji, M. (2022) ‘Environmental applications of phytonanotechnology: A promise to sustainable future’, Phytonanotechnology, pp. 141–159. doi:10.1007/978-981-19-4811-4_7.

[3]. Chen, C.-H., Lin, Y.-C. and Yen, F.-S. (2021) ‘Synthesis and characterization of conducting PANDB/χ-al2o3 core-shell nanocomposites by in situ polymerization’, Polymers, 13(16), p. 2787. doi:10.3390/polym13162787.

[4]. ElFaham, M.M., Okil, M. and Mostafa, A.M. (2020) ‘Fabrication of magnesium metallic nanoparticles by liquid-assisted Laser Ablation’, Journal of the Optical Society of America B, 37(9), p. 2620. doi:10.1364/josab.398543.

[5]. Choudhari, K.S. et al. (2018) ‘Influence of electrolyte composition on the photoluminescence and pore arrangement of nanoporous anodic alumina’, ECS Journal of Solid State Science and Technology, 7(11). doi:10.1149/2.0081811jss.

[6]. Choudhari, U. and Jagtap, S. (2022) ‘Lanthanum doped tin oxide: Synthesis, characterization and application’, Materials Today: Proceedings, 49, pp. 3325–3330. doi:10.1016/j.matpr.2021.01.129.

[7]. Chu, H., Shi, W., et al. (2022) ‘Feasibility of manufacturing self-compacting mortar with high elastic modulus by Al_2O_3 micro powder: A preliminary study’, Construction and Building Materials, 340, p. 127736. doi:10.1016/j.conbuildmat.2022.127736.

[8]. Chu, H., Wang, Q., et al. (2022) ‘An approach of producing ultra-high-performance concrete with high elastic modulus by Nano-Al2O3: A preliminary study’, Materials, 15(22), p. 8118. doi:10.3390/ma15228118.

[9]. Cuong, H.N. et al. (2022) ‘New frontiers in the plant extract mediated biosynthesis of copper oxide (Cuo) nanoparticles and their potential applications: A Review’, Environmental Research, 203, p. 111858. doi:10.1016/j.envres.2021.111858.

[10]. Dalvand, R. et al. (2020) ‘MgO nano-sheets for adsorption of anionic dyes from aqueous solution: Equilibrium and Kinetics Studies’, Surfaces and Interfaces, 21, p. 100722. doi:10.1016/j.surfin.2020.100722.

[11]. Dhabale, R.B. et al. (2023) ‘Friction stir welding of dissimilar materials with reinforcement of copper particulates’, Key Engineering Materials, 941, pp. 3–10. doi:10.4028/p-ltn695.

[12]. G. P. Zhang et al., 2019 ‘Production of a high strength Al/(TiAl3 +Al2O3) composite from an Al-TiO2 system by accumulative roll-bonding andspark plasma sintering’ Mater. Sci. Eng. A, vol. 752, no. February, pp. 192–198, , doi:10.1016/j.msea.2019.03.012.

[13]. K, Preethi., T.N, R. and H.A, S. (2021) ‘Development and characterization of carbon nanotube reinforced aluminium-6061 metal matrix composites’, Journal of Minerals and Materials Characterization and Engineering, 09(03), pp. 290–300. doi:10.4236/jmmce.2021.93020.

[14]. Filali, H. et al. (2021) Improvement of the optical and photocatalytic properties of ZNAL2O4: 1% La3+, x% pb2+ nanoparticles synthesized by citrate sol-gel route [Preprint]. doi:10.21203/rs.3.rs-316386/v1.

[15]. G, S. et al. (2022) ‘Green and chemical synthesis of Cuo nanoparticles: A comparative study for several in vitro bioactivities and in vivo toxicity in zebrafish embryos’, Journal of King Saud University - Science, 34(5), p. 102092. doi:10.1016/j.jksus.2022.102092.

[16]. G. P. Zhang et al., 2019 ‘Production of a high strength Al/(TiAl3 +Al2O3) composite from an Al-TiO2 system by accumulative roll-bonding andspark plasma sintering’ Mater. Sci. Eng. A, vol. 752, no. February, pp. 192–198, , doi:10.1016/j.msea.2019.03.012.

[17]. Ghafaripoor, M. et al. (2018) ‘The corrosion and tribocorrosion resistance of PEO composite coatings containing α-al2o3 particles on 7075 Al Alloy’, Surface and Coatings Technology, 349, pp. 470–479. doi:10.1016/j.surfcoat.2018.06.027.

[18]. Ghariani, F., Fezei, R. and Hamzaoui, A.H. (2018) ‘Synthesis, characterization, and application of Sol Gel derived mg2sio4 powder’, Journal of Sol-Gel Science and Technology, 88(1), pp. 100–104. doi:10.1007/s10971-018-4736-5.

[19]. Ghosal, P.S. and Gupta, A.K. (2018) ‘Thermodynamics of fluoride adsorption on aluminum/olivine composite (AOC): Influence of temperature on isotherm, kinetics, and adsorption mechanism’, Water, Air, & Soil Pollution, 229(11). doi:10.1007/s11270-018-4003-y.

[20]. Gupta, R. et al. (2020) ‘A comparative study of dry sliding wear behaviour of sillimanite and rutile reinforced LM27 aluminium alloy composites’, Materials Research Express, 7(1), p. 016540. doi:10.1088/2053-1591/ab61a2.

[21]. Gupta, R., Nanda, T. and Pandey, O.P. (2022) ‘Tribological properties of hybrid aluminium matrix composites reinforced with boron carbide and ilmenite particles for brake rotor applications’, Archives of Civil and Mechanical Engineering, 23(1). doi:10.1007/s43452-022-00569-4.

[22]. H. Liao, J. Zhu, S. Chang, G. Xue, H. Zhu, and B. Chen, (2020) “Al2O3 loss prediction model of selective laser melting Al2O3–Al composite,” Ceram. Int., vol. 46, no.9, pp. 13414–13423, doi:10.1016/j.ceramint..02.124.

[23]. Hakimi, M. et al. (2019) ‘Preparation, characterization, and photocatalytic activity of bi2o3–al2o3 nanocomposite’, Polyhedron, 170, pp. 523–529. doi:10.1016/j.poly.2019.06.029.

[24]. Hakimyfard, A., Zalpour, N. and Zarinabadi, F. (2022) ‘Physical properties and photocatalytic activity of new classes of MX-ZnO-Bi2O3-WO3 and MX-ZnO-Bi2O3-MoO2 (M = none, Fe, Co, and ni) nanocomposites’, Journal of the Australian Ceramic Society, 58(3), pp. 817–830. doi:10.1007/s41779-022-00727-0.

[25]. He, J. et al. (2020) ‘Ce(iii) nanocomposites by partial thermal decomposition of CE-MOF for effective phosphate adsorption in a wide ph range’, Chemical Engineering Journal, 379, p. 122431. doi:10.1016/j.cej.2019.122431.

[26]. Hua, A. et al. (2022) ‘Fabrication, microstructure characterization and mechanical properties of B4C microparticles and sic nanowires hybrid reinforced aluminum matrix composites’, Materials Characterization, 193, p. 112243. doi:10.1016/j.matchar.2022.112243.

[27]. Ibrahim, A.F., Mousa, S.M. and Noori, D.A. (2022) ‘Investigation and optimization of machining parameters in electrochemical machining of Aluminium Metal Matrix Composites’, Periodicals of Engineering and Natural Sciences (PEN), 10(3), p. 48. doi:10.21533/pen.v10i3.3006.

[28]. Islam, M. et al. (2022) ‘Machining performance of Nano Sic and graphite powder mixed aluminum matrix composites fabricated by powder metallurgy using EDM’, Materials Today: Proceedings [Preprint]. doi:10.1016/j.matpr.2022.11.123.

[29]. Jiang, X., Xiao, D. and Teng, X. (2022) ‘Influence of vibration parameters on ultrasonic vibration cutting micro-particles reinforced SIC/Al Metal Matrix Composites’, The International Journal of Advanced Manufacturing Technology, 119(9–10), pp. 6057–6071. doi:10.1007/s00170-021-08525-x.

[30]. Joshi, A. et al. (2019) ‘Plant-mediated synthesis of copper oxide nanoparticles and their biological applications’, Nanomaterials and Plant Potential, pp. 221–237. doi:10.1007/978-3-030-05569-1_8.

[31]. Jyoti and Kumar, R. (2022) 'Investigation of effect of spinning speed on structural, electrical and optical properties of Cuo Thin Films prepared by sol–gel spin coating technique', Journal of Optics [Preprint]. doi:10.1007/s12596-022-00942-9.

[32]. K, Preethi., T.N, R. and H.A, S. (2021) 'Development and characterization of carbon nanotube reinforced aluminium-6061 metal matrix composites', Journal of Minerals and Materials Characterization and Engineering, 09(03), pp. 290–300. doi:10.4236/jmmce.2021.93020.

[33]. Kantharia, M. and Kumar Mishra, P. (2021) 'Investigation on compressive strength of cement mortar with Nano Alumina', Materials Today: Proceedings, 47, pp. 7181–7183. doi:10.1016/j.matpr.2021.06.410.

[34]. Karthik H.G., S. et al. (2019) 'Effect of zn substitution in cr3+ doped MgAl2O4 mixed spinel nanoparticles on red/nir emission properties', Materials Research Bulletin, 111, pp. 294–300. doi:10.1016/j.materresbull.2018.11.035.

[35]. Kasirajan, K. and Karunakaran, M. (2019) 'Synthesis and characterization of strontium cerium mixed oxide nanoparticles using plant extract', Sensor Letters, 17(12), pp. 924–937. doi:10.1166/sl.2019.4166.

[36]. Kassahun, F. et al. (2023) 'Magnetic al2o3/zro2/FE3O4 nanocomposite: Synthesis, characterization, and application for the adsorptive removal of nitrate from aqueous solution', Groundwater for Sustainable Development, 20, p. 100873. doi:10.1016/j.gsd.2022.100873.

[37]. Kaveri, N. and Balavijayalakshmi, J. (2020) 'Impact of molybdenum on structural and morphological properties of manganese ferrite nanoparticles by hydrothermal method', Materials Today: Proceedings, 33, pp. 2390–2395. doi:10.1016/j.matpr.2020.06.442.